An original DEM bearing model with electromechanical coupling

C. Machado[1,a)], S. Baudon[1,4], M. Guessasma[1], V. Bourny[1,2], J. Fortin[1,2], R. Bouzerar[3]and P. Maier[4]

[1]Laboratoire des Technonologies Innovantes (LTI EA3899), Université de Picardie Jules Verne, France

[2]ESIEE Amiens, 4 quai de la Somme, 80082 Amiens Cedex 2, France

[3]Laboratoire de Physique de la Matiére Condensée (LPMC EA2081), Université de Picardie Jules Verne, France

[4]société EREM, ZA Sud, Rue de la sucrerie, 60130 Wavignies, France

[a)]Corresponding and presenting author: charles.machado@u-picardie.fr

ABSTRACT

Rolling bearings are one of the most important and frequently components encountered in domestic and industrial rotating machines. Statistical studies show that these bearings are considered as critical mechanical parts which represent between 40% and 50% of malfunction in rotating machineries. We performed an electrical monitoring of a bearing and numerical aspects using smooth contact dynamic are studied. An original elastic 2D modelling by discrete elements (DEM) reproduces the dynamic and the mechanical behavior of a bearing [1]. An electromechanical coupling is introduced to provide monitoring solutions [2]. This study proposes an original method of simulating the bearings to analyze dynamic stress in rings and to detect malfunctions (defects or unusual load) in the impedance of a ball bearing over time. The bearing is seen as a polydisperse granular chain where rolling elements and cage components interact with a Hertzian contact model. Moreover, rings (and housing) are also taken into account using a cohesive model [3]. Indeed, while many studies have been conducted on bearing simulation using FEM and multibody approaches, this new discrete model gives relevant information on physical phenomena in the contact interface. Roller-race contacts are analyzed in detail with an electromechanical coupling. One of our objectives is to investigate the sensitivity of the electrical measurement due to the variation of mechanical loading.

Keywords: bearing, electromechanical coupling, DEM, electrical transfer, contact model, roughness

Introduction

Rolling elements bearings are among the most important components in rotating machinery. In order to ensure the industrial systems availability and the safety of goods and persons, the monitoring and diagnosis of bearing defects have to be considered with prime importance and the challenges in terms of productivity are non-negligible. Recently, maintenance has led to extensive research with the development of new methods. Usually, vibrations and sounds of the machine are followed over time with a sensor and coupled analysis of time domain and frequency domain give information about the bearing state [4, 5]. Thermal and current motor analysis may be implemented to confirm the presence of abnormalities. A detected defect means that the damage is already sufficiently pronounced to be corrected and the bearing has to be changed. Finally, a defect is often due to mounting problem which implies unbalanced load, excessive load, misalignment... In this paper, a mechanical comparison between rigid housing and elastic housing is discussed. The rigid assumption becomes unrealistic when the machine design is optimized to minimize congestion and to reduce costs in raw material. Knowledge of the state of load bearing is particularly important but in practice, it is difficult to determine the loading bearing accurately. A new tool based on electrical measurements is presented in order to monitor the loads before problems occurs. Moreover, this electrical measurement has proven itself for a low speed application where other measurements are difficult to implement. A test bench has allowed to find some sensitivities relative to a charge status in the electrical measurement[6]. Although, the presence of an electric current through the ball bearing is ordinary harmful but the current densities required to perform a relevant experimental measurement are sufficiently low to cause damage [7, 8]. While most numerical studies on the bearing are carried out with finite

elements (FEM) [9, 10] and multibody approaches [11, 12], an original numerical approach using discrete element method is described in this paper and dynamic electromechanical simulations are studied. These developments are a straight continuation of previous work initiated in [13, 14] with notable advances in rings modelling.

DEM Mechanical modelling

A ball bearing is made of rolling elements constrained by two rings. A cage ensures a constant space between each rolling element. This component is seen as a granular chain. To distinguish themselves from multibody and FEM approaches, some important mechanical considerations are modelled in this paper and a dynamical resolution is proposed. The cage component is made of discrete elements moving freely along the pitch radius ($R_{pich} = \frac{R_{race}^{inner} + R_{race}^{outer}}{2}$) and the rings and the housing are elastic. The rings can be deformed under mechanical load if the housing is sufficiently flexible. In this original description, a bearing is represented by a collection of polydispersed (cylindrical or spherical) rigid particles. Contact interactions with particles are given with a contact model for the interface description and with a cohesive model for the continuum media (figure 1). A

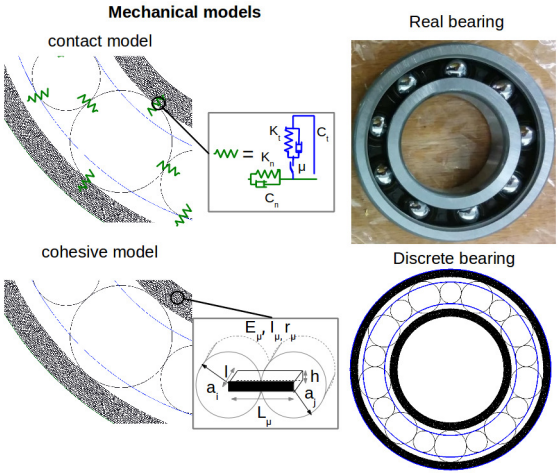

Figure 1. General mechanical modelling

commonly used radial ball bearing type 6208 is selected for modelling and its dimensions are given in table 2 :

$R_{rolling}$	R_{cage}	R_{race} inner	R_{race} outer	inner ring thickness	outer ring thickness
0.0063 m	0.0042 m	0.024 m	0.0366 m	0.003 m	0.003 m

Figure 2. Dimensions of a radial ball bearing 6208

Contact description

By using the smooth contact DEM, developed by Cundall and Strack [15, 16], the contact forces in a bearing are described with a contact model depending on elastic force displacement law, Coulomb's friction and viscous damping. The principle of the calculation is based on dynamic considerations and the contact occurs only when particles penetrate which means that a contact between a rolling element and a ring or a contact between a rolling element and a cage component is proved. The equivalent model of the contact is given in figure 1 using analogies with damped springs mass systems (K_n, K_t, C_n and C_t) and the dry friction coefficient μ, set to $\mu = 0.1$ are introduced. The lubricant effect is not taken into account and a rough interface is modelled [17]. The force $\vec{F_i}$ between particles at the interface includes the inter-particle interaction forces and the external forces.

$$\vec{F_i} = \sum_{j \neq i} \vec{F_{ij}} + \vec{F_{ext,i}} \tag{1}$$

Where $\vec{F_{ij}}$ is the force exerted by particle j to particle i. $\vec{F_{ext,i}}$ are the external forces on particle i (gravity, loading, ...). The contact force $\vec{F_{ij}}$ is deduced from analogies with damp-spring. From figure (1), this model includes a normal component and a tangential component. $\vec{F_{ij}}$ is then decomposed as follow :

$$\vec{F_{ij}} = F_n\vec{n} + F_t\vec{t} \tag{2}$$

F_n is the contact force in the normal direction and F_t is the contact force in the tangential direction. By considering the analogies with a damped spring mass system, where K_n,C_n and K_t, C_t represent the stiffness and the viscous damping coefficient, in the normal direction $\vec{n}$ and in the tangential direction $\vec{t}$. The overlap between particles $\vec{u} = u_n\vec{n} + u_t\vec{t}$ gives the contact force :

$$\begin{cases} F_n = K_n \times u_n + C_n \times \vec{u}.\vec{n} \\ F_t = K_t \times u_t + C_t \times \vec{u}.\vec{t} \end{cases} \tag{3}$$

where $\vec{u}$ is the relative velocity of the contact point between particles. The tangential overlap u_t can be approximated by the expression : $u_t = \vec{u}.\vec{t}\Delta_t$, where Δ_t is the time step. F_t is a candidate force because the slider μ, due to dry friction is considered. Coulomb's friction law is written in equation 4 and determines whether the contact is slipping or sliding :

$$F_t = -min(F_t, \mu F_n) \times sgn(\vec{u}.\vec{t}) \tag{4}$$

The expressions of normal and tangential stiffness are given from the elastic solid mechanics analysis of Hertz-Mindlin theory [18, 19] :

$$\begin{cases} K_n = 4E\dfrac{a_i a_j}{a_i + a_j} \\ K_t = K_n \dfrac{1-\nu}{1-\frac{1}{2}\nu} \end{cases} . \tag{5}$$

K_n and K_t are related to mechanical properties the Young's modulus E, the Poisson's ratio ν and the dimensions of particles in contact (a_i, a_j). The harmonic behaviour of linear model with constant parameters is well known and adapted in a first approximation for a description of a roller bearing. A general load-deflection relationship without damping is written as $F_n = K_n U_n^N$, where N and K_n depend on the bearing type ($N = 10/9 \sim 1$ for a roller-raceway contact, $N = 3/2$ for a ball-raceway contact, ...). The role of interactions at the contact plays an important role in the distribution of efforts. Harris [20] offers similar stiffness models derived from Hertz's theory. A critical viscous damping ratio $C_{n,t}$ is introduced by equation 6, where m^* is the reduced mass :

$$C_{n,t} = 2\sqrt{K_{n,t}m^*} \tag{6}$$

Other viscous damping coefficients can be introduced if lubricant effects are considered [21, 22]. A simple bearing is made of $2Z + 1$ discrete elements where Z are dedicated to rolling elements, Z others are dedicated to cage components and the last one represents the inner race/ring or shaft.

Cohesive description

Rings and the housing may be deformed under mechanical loadings. In order to simulate a 2D continuous material with DEM, the rings are discretized by a dense polydisperse granular assembly. The generation is controlled with Lubachevsky-Stillinger's algorithm [23] so as to satisfy the following properties :

- Isotropic contact orientation
- Local homogeneous properties (coordination number, local porosity, ...)
- Compacity close to 86-87 % (Random close packing [24])

In order to reflect the mechanical behaviour of continuous medium, contacts must be persistent and a cohesive contact law is considered (figure 1). In the proposed DEM formulation, the interaction between two particles in contact is modelled with a beam of length L_μ, Young's modulus E_μ, cross-section A_μ and quadratic moment $I\mu$ (figure 1) [25]. Therefore, the cohesive contacts are maintained by a vector of three-component generalized forces acting as internal forces. The normal component acts as an attractive or repulsive force, the tangential component allows to resist to the tangential relative displacement and the moment component counteracts the

bending motion.
From figure 1, A_μ is rectangular with depth $l = 1cm$ and h, the height of the cross section defined by :

$$h = r_\mu \frac{a_i + a_j}{2} \tag{7}$$

where $r_\mu \in]0, 1]$ is a dimensionless radius, a_i and a_j are respectively the radius of particles i and j. The cohesive forces and moments between two particles i and j are given as follow:

$$\begin{cases} m_i \ddot{u}_i = F_i^{ext} + \sum_j F^{i \to j} \\ I_i \ddot{\theta}_i = M_i^{ext} + \sum_j M^{i \to j} \end{cases} \tag{8}$$

where m_i is the elementary matrix and I_i is the quadratic moment of intertia of the particle i. $F^{i \to j}$ and $M^{i \to j}$ are respectively the force and the moment of interaction of particle j on i. F^{ext} et M^{ext} are respectively the external force and moment of acting on particle i.
The local cohesion forces between particles i and j are deduced from the following linear system :

$$\begin{bmatrix} F_n^{i \to j} \\ F_t^{i \to j} \\ M_{i \to j}^{int} \end{bmatrix} = \begin{bmatrix} \frac{E_\mu A_\mu}{L_\mu} & 0 & 0 & 0 \\ 0 & \frac{12 E_\mu I_\mu}{L_\mu^3} & \frac{6 E_\mu I_\mu}{L_\mu^2} & \frac{6 E_\mu I_\mu}{L_\mu^2} \\ 0 & \frac{6 E_\mu I_\mu}{L_\mu^2} & \frac{4 E_\mu I_\mu}{L_\mu} & \frac{2 E_\mu I_\mu}{L_\mu} \end{bmatrix} \begin{bmatrix} u_n^i - u_n^j \\ u_t^i - u_t^j \\ \theta_i \\ \theta_j \end{bmatrix}$$

where θ_i and θ_j are respectively the rotations of particles i and j. $u_n^{i,j}$ and $u_t^{i,j}$ are respectively the normal and tangential displacements. The numerical resolution is based on an explicit time integration with a formulation based on a Verlet scheme. In the ball bearing context, the rings are made of steel and the identification of model parameters E_μ and r_μ is correlated with macroscopic Young's modulus $E_M = 210GPa$ and Poisson's ratio $\nu_M = 0.3$. A procedure based on a uniaxial quasi-static tensile test [26] suggests to choose $E_\mu = 505GPa$ and $r_\mu = 0.5$. The rings and the housing are composed of millimeter polydisperse particles.

Electromechanical modelling

The electrical transfer in a bearing in operation is a complex mechanism depending on intrinsic mechanical, electrical properties of materials in contact and on properties of the interface (roughness, lubricant film, oxydation, temperature, ...). Electrical response depends also on mechanical load and on rotation speed. For moderate rotation speeds ω and heavy loads F_r, the lubricant thickness in the interface may be neglected [6] and a simple electrical model, based on analogies with resistors is considered [2, 13, 14]. We assumed that the temperature is constant and the oxyde layer on the surface of particles is neglected but the effect of roughness is considered. An electrical macroscopic resistance is associated to each rolling element in contact with both rings using expression 9 :

$$\frac{1}{R_{ij}^k} = \frac{\gamma S_i S_j}{2V_b}(1 - cos\theta) \tag{9}$$

where γ is the electrical conductivity of steel ($\gamma = 5.8 \times 10^7 S.m^{-1}$), V_b is the volume of the rolling element, θ is the angle formed by the points i and j ($\theta = \pi$ for radial bearings). The coupling between the mechanical and electrical computation is carried out by Hertz's theory where S_i and S_j denote contact areas. The elements of the cage are insulating (made of polyamide) therefore only the rolling elements are involved in current transfer. Considering a cohesive model implies rough races depending on the discretization. The contact between a rolling element and a race is supported by small cohesive particles. This description of rough contact using spherical caps can be found in the Greenwood's work [27, 28]. Unlike previous works where a perfect contact was considered leading to overly conductive simulations [14], the contact area responsible of the electrical transfer is the sum of spots using Hertz's theory, as suggested by figure 3(b). The surface of rolling elements is supposed perfect but in practice the arithmetical rugosity of a rolling element ($Ra_b = 10^{-8}$ m) is about ten time smaller than the arithmetical rugosity of races ($Ra_{race} = 10^{-7}$ m). The roughness is numerically overestimated for reasons of time computing.

For a rolling element k, at the angular position ψ^k, the radial local load Q_ψ^k is distributed over several "micro-contacts" or spots on the inner race (or outer race), as shown in figure 3(b). The contact area responsible of

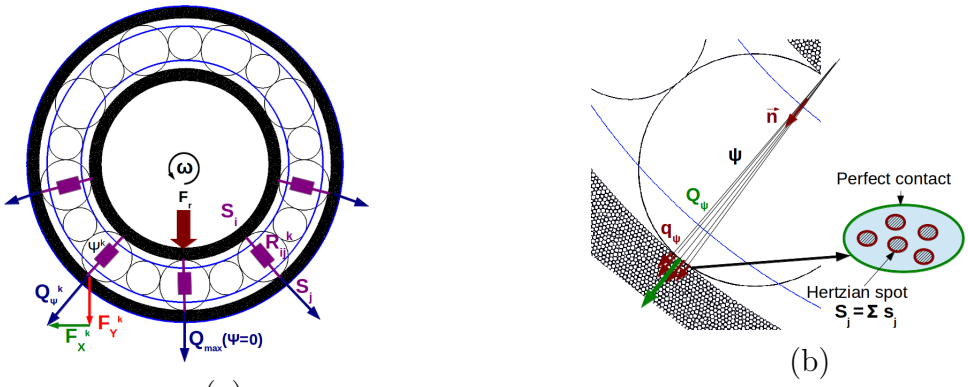

(a) (b)

Figure 3. (a) Load projection and electrical circuit (b) interface description

the electrical transfer is written as follow :

$$S = \sum_{i=1}^{m_c} s_i = \sum_{i=1}^{m_c} \pi \left(\frac{3 \times q_\psi^i R^*}{4E^*} \right)^{2/3} \tag{10}$$

where m_c is a number of "micro-contact" within a contact between a rolling element and a ring, depending on the discretization. q_ψ^i denotes the radial load transmitted by the "micro-contact" i. R^* and E^* respectively characterize the relative radius of curvature and the reduce modulus.

Simulation results

The electromechanical results are obtained for a fixed rotation speed $\omega = 500$ rad/s and the time step is $\Delta_t = 10^{-8}$ s. The considered bearing has no clearance which means that only 50 % of rolling elements are implicated in the electrical determination. The rolling components in the load zone form a parallel electrical resistor circuit, as shown in figure 3(a).

Mechanical analysis

Consider a bearing with rigid rings or deformable rings involves particular mechanical behaviours that affect the bearing fatigue lifetime and the electrical determination. The rigid description is made of $26100 + 19$ discrete elements and the elastic description is made of $36100 + 19$ discrete elements (figure 4(a)).

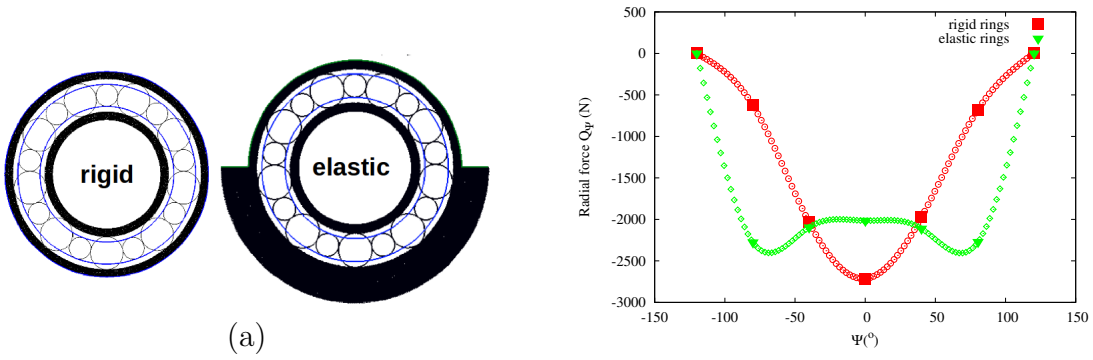

(a) (b)

Figure 4. (a) DEM models (b) Static radial load distribution for $F_r = 6$ kN

A radial load $\vec{F_r}$ = -6 $\vec{j}$ kN is applied on the inner ring according to the vertical direction. From figure 4(b), at the static equilibrium ($\omega = 0$), the local load distribution Q_ψ is represented according to angular position ψ, in rigid and elastic cases. Each point (■ or ▼) gives the position and the radial local load supported by a

rolling element and points ($\diamondsuit$ or $\odot$) give typical trends. The radial load distribution with rigid rings describes a sinusoid function which matches with the classical rigid theory [20] :

$$Q_\psi = Q_{max}\left(1 - \frac{1}{2\epsilon}(1 - cos\psi)\right)^N \tag{11}$$

where $Q_{max} \sim -2728$ N denotes the maximum radial local load at $\psi = 0°$ and for a roller bearing Q_{max} may also be determined using radial integral $J_r(\epsilon)$ with expression $Q_{max} = \dfrac{J_r(\epsilon = 0.5) \times F_r}{Z} = \dfrac{4.08 \times -6000}{9} = -2720$ N. The dimensionless load parameter ϵ describes the state of load. When no clearance or preload is considered, $\epsilon = 0.5$ means over half of rolling elements is involved in the radial distribution. N is relative to the stiffness model ($N = 3/2$ for ball bearing and $N \sim 1$ for roller bearing. The radial load distribution with elastic rings shows a symmetrical function about the vertical axis where $Q_{max} \sim -2250$N is found at angle $\psi \pm 80°$, caused by the roundness of the rings. There is no theoretical expression associated with this elastic distribution.

The following simulations are obtained by considering a non-zero rotational speed $\omega = 500 rad/s$. The static equilibrium described in figure 4(b) is replaced by complex dynamic regime where deformation modes of the rings and rough interfaces disturb the load distribution over time as suggested by figures 5.

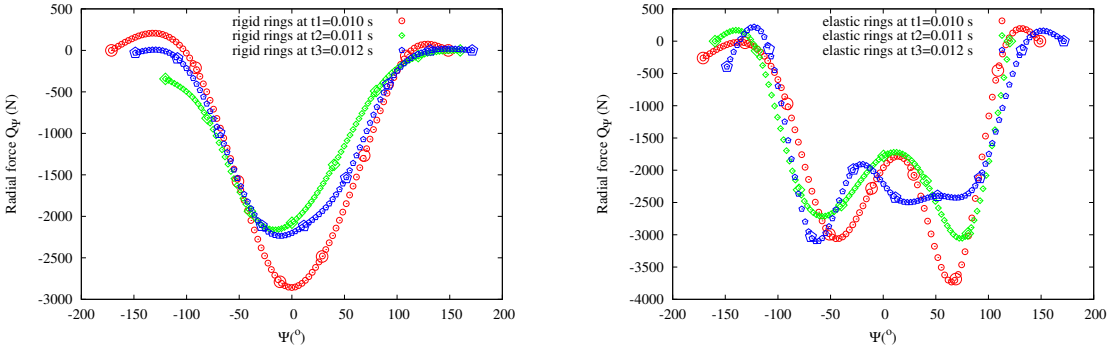

(a) (b)

Figure 5. Radial load distribution for several instants at $F_r = 6$ kN and $\omega = 500$ rad/s (a) for rigid rings (b) for elastic rings

The rigid results over time show that the sinusoidal profile conserves the same shape and Q_{max} is time varying due to micro-contact variations. A similar analysis could be done for elastic results. These remarks demonstrate that even if a constant load F_r and a constant rotation speed ω are applied to the system, the mechanical response in the bearing is time varying. The main difference between rigid and elastic analysis, in dynamic or static attempts to show that areas prone to damage are dependent on the rigidity of the montage. As proof, the dynamical study of mechanical stress fields in the rings at same time (figure 6) shows that in the rigid case, the area or contact interface near the south pole ($\psi = 0$) is more prone to damages. In the elastic case, this area is pushed towards the embedding conditions close to $\psi \pm 90°$.

Electrical analysis

The electrical sensitivity over time is simulated for several radial load F_r at 50 kHz. The overall electrical resistance is given in figure 7(a) for rigid rings and in figure 7(b) for elastic rings.

In both cases, when the radial load F_r increases, the electrical resistance decreases with a non linear dependency according to Hertz's theory [14]. Typical values of the electrical resistance computed which may be assimilated to the mean resistances give the order of Ω. In rigid considerations, the resistance shows substantial variations in amplitude depending on load at high frequencies due to micro-contact variation (figure 7(a)). In flexible considerations, the micro-contact variation still exists but due to the elasticity of the system, the resistance is less noisy and a typical low frequency appears close to 300 Hz (figure 7(b)). This low frequency is assumed to

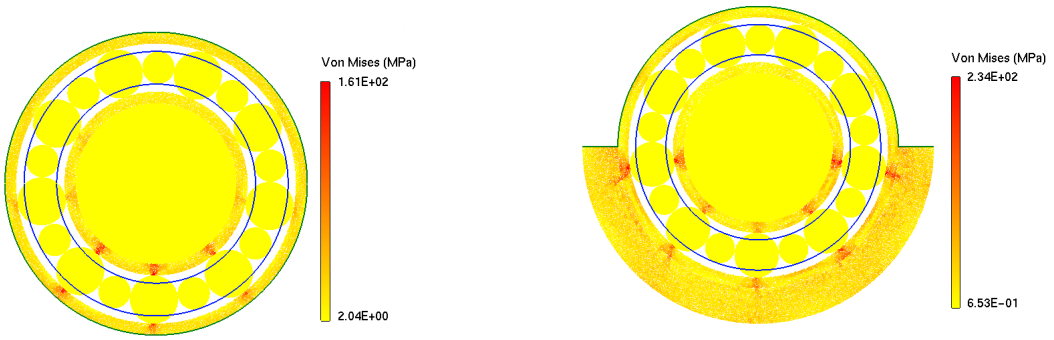

(a) (b)

Figure 6. Von Mises stress in a bearing at $F_r = -6$ kN and $\omega = 500$ rad/s (a)with rigid rings (b) with elastic rings

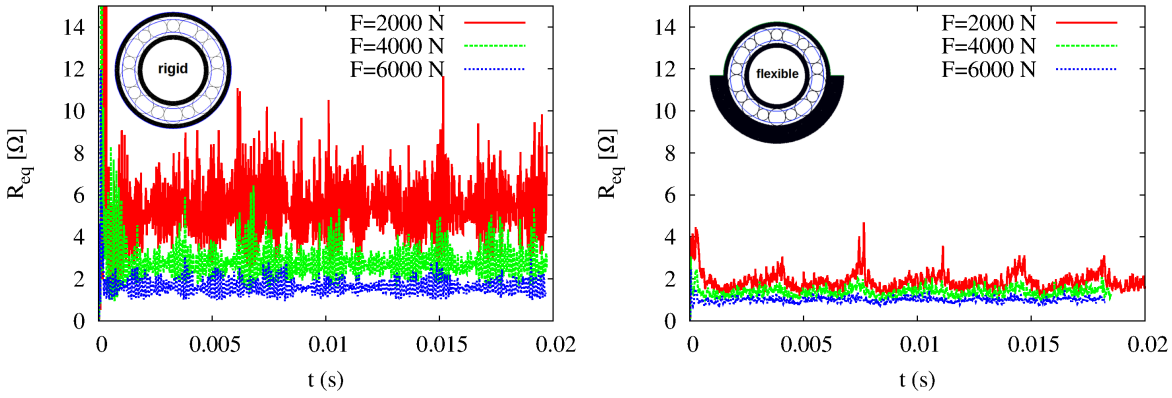

(a) (b)

Figure 7. Electrical resistance versus time with different radial loads F_r at $\omega = 500$ rad/s (a) for rigid rings (b) for elastic rings

be related to the system deformation modes. For an identical radial load, the flexible mounting systematically gives a lower resistance than the rigid case.

Conclusion

An original description of the dynamic behaviour of bearings with DEM is described and interesting electromechanical results are discussed. This type of modelling provides access to new quantities for understanding the mechanisms of damage (figure 6). Load distribution of the bearing is determined with a contact law based on analogies with damped springs and deformations of rings using a cohesive model are considered. In a static case with rigid rings, the contact model K_n verifies Harris's theory [20] and taking account of the rigidity of the rolling bearing implies significant effects. An electrical measurement is proposed to diagnose the state of load in operation. The electrical sensitivity of this measurement allows us to distinguish several radial loads. Subsequently, abnormal loads, misalignments and defects generated with decohesion will be imposed on ball bearings and their electrical signatures will be analysed. For now, the electrical model considers a rough contact but we could improve this model by taking into account the effect of lubricant with the theory of elastohydrodynamic lubrication [29]. In this case, the lubricant acts as a capacitor and an electrical model based on impedance spectroscopy has to be developed. In a future work, simulation results will be compared with experimental measurements for moderate speeds. Other simulations on a elementary rolling contact will introduce realistic roughness.

Acknowledgements : *This study has been carried out under project EROLLING2 (2015-2018) using the univer-*

sity Chair program on electrical transfer. Thanks to the "Région Nord-Pas de Calais-Picardie" for its financial support.

References

[1] K. Bourbatache, M. Guessasma, E. Bellenger, V. Bourny, and A. Tekaya. Discrete modelling of electrical transfer in multi-contact systems. *Granular Matter*, 14 (1):1–10, 2012.

[2] C. Machado, M. Guessasma, E. Bellenger, K. Bourbatache, V. Bourny, and J. Fortin. Diagnosis of faults in the bearing by electrical measures and numerical simulations. *Mechanics and Industry*, 15(5):383–391, 2014.

[3] H. Haddad. *Couplage MED-MEF : modélisation numérique du transfert thermique dans les interfaces de contact.* PhD thesis, Université de Picardie Jules Verne, 2013.

[4] R. B. Randall and J. Antoni. Rolling element bearing diagnostics - a tutorial. *Mechanical Systems and Signal Processing*, 25:485–520, 2011.

[5] N. Tandon and A. Choudhury. A review of vibration and acoustic measurement methods for the detection of defects in rolling element bearings. *Tribology International*, 32(8):469–480, 1999.

[6] C. Machado. *Modélisation et simulation éllectromélcaniques par la MED des systèmes multi-contacts : application à la surveillance des roulements par une mesure électrique.* PhD thesis, Université de Picardie Jules Verne, 2015.

[7] J.R. Stack, T.G. Habetler, and R.G. Harley. Experimentally generating faults in rolling element bearings via shaft current. *IEEE transactions on industry applications*, 41 (1):25–29, 2005.

[8] D.F. Busse, J.M. Erdman, R.J. Kerkman, D.W. Schlegel, and G.L. Skibinski. The effects of pwm voltage source inverters on the mechanical performance of rolling bearings. *IEEE transactions on industry applications*, 33 (2):567–576, 1997.

[9] N. Demirhan and B. Kanber. Stress and displacement distributions on cylindrical roller bearing rings using fem. *Mechanics Based Design of Structures and Machines*, 36:86–102, 2008.

[10] A. E. Azianou, K. Debray, F. Bolaers, P. Chiozzi, and F. Palleschi. Modeling of the behavior of a deep groove ball bearing in its housing. *Journal of Applied Mathematics and Physics*, 1:45–50, 2013.

[11] M. Tiwari and K. Gupta. Dynamic response of an unbalanced rotor supported on ball bearings. *Journal of Sound and Vibration*, 238 (5):757–779, 2000.

[12] L. Xu, Y. Yang, Y. Li, C. Li, and S. Wang. Modeling and analysis of planar multibody systems containing deep groove ball bearing with clearance. *mechanism and machine theory*, 56:69–88, 2012.

[13] K. Bourbatache, M. Guessasma, E. Bellenger, V. Bourny, and J. Fortin. Dem ball bearing model and defect diagnosis by electrical measurement. *mechanical systems and signal processing*, 41:98–112, 2013.

[14] C. Machado, M. Guessasma, and E. Bellenger. Electromechanical modelling by dem for assessing internal ball bearing loading. *Mechanism and Machine Theory*, 92:338–355, 2015.

[15] O. D. L. Cundall and P. A. Strack. A discrete numerical model for granular assemblies. *Géotechnique*, 29:235–257, 1979.

[16] P. A. Cundall. Formulation of three-dimensional distinct element mode part 1. a scheme to detect and represent contacts in a system composed of many polyhedral blocks. *J. Rock Mech., Min. Sci. and Geomech*, 25:107–116, 1988.

[17] R. Stribeck. Ball bearings for various loads. *Trans. ASME*, 29:420–463, 1907.

[18] H. Hertz. "uber die beruhrung fester elastischer korper" on the contact of elastic solids. *reprinted in Miscellaneous Papers, Macmillan*, pages 146–162, 1896.

[19] R. D. Mindlin and H. Deresiewicz. Elastic spheres in contact under varying oblique force. *ASME journal of applied mechanics*, 20:327–344, 1953.

[20] T. A. Harris and M. N. Kotzalas. *Rolling Bearing Analysis : Essential concepts of Bearing Technology.* 2006.

[21] D. Downson and G. R. Higginson. *Elasto-hydrodynamic lubrication.* Pergamon Press, 2nd ed, 1977.

[22] B. J. Hamrock and W. J. Anderson. Analysis of an arched outer race ball bearing considering centrifugal forces. *ASME Journal of Tribology*, 95 (3):265–276, 1973.

[23] B. D. Lubachevsky and F. H. Stillinger. Geometric properties of random disk packings. *Journal of Statistical Physics*, 60 (5):561–583, 1990.

[24] G. D. Scott and D. M. Kilgour. The density of random packing of spheres. *Appl. Phys.*, 2:863–866, 1969.

[25] D. André, I. Iordanoff, J.-L. Charles, and J. Néauport. Discrete element method to simulate continuous material by using the cohesive beam model. *Comput. Methods Appl. Mech. Engrg*, 213-216:113–125, 2012.

[26] H. Haddad, W. Leclerc, M. Guessasma, C. Pélegris, E. Bellenger E., and N. Ferguen. Application of dem to predict the elastic behavior of particulate composite materials. *Granular Matter*, 17 (2):459473, 2015.

[27] J. A. Greenwood and J. B. P. Williamson. Contact of nominally flat surfaces. *Proc. of the Royal A.*, 295:300–319, 1966.

[28] J. A. Greenwood. Constriction resistance of the real area of contact. *Brit. J. Appl. Phys.*, 17, 1966.

[29] B. J. Hamrock and W. J. Anderson. *Rolling-element bearings.* National Technical Information Service, 1983.